Scientific Research Publishing

International Journal of Geosciences, 2022, 13, 319-328
https://www.scirp.org/journal/ijg
ISSN Online: 2156-8367
ISSN Print: 2156-8359

Applications of Amplitude versus Offset and Seismic Attributes for Perceiving Messinian Reservoirs in Nidoco Field, Nile Delta, Egypt

Ahmed Abu El-Saoud[1*], Abd El-Nasser Helal[2], Justin Matresu[3], Amir M. S. Lala[2*]

[1]Belayim Petroleum Company (Petrobel), Cairo, Egypt
[2]Faculty of Science, Ain Shams University, Cairo, Egypt
[3]Exploration Team Leader at Eni, Cairo, Egypt
Email: *amir77_lala@yahoo.com

How to cite this paper: El-Saoud, A.A., El-Nasser Helal, A., Matresu, J. and Lala, A.M.S. (2022) Applications of Amplitude versus Offset and Seismic Attributes for Perceiving Messinian Reservoirs in Nidoco Field, Nile Delta, Egypt. *International Journal of Geosciences*, **13**, 319-328.
https://doi.org/10.4236/ijg.2022.135017

Received: February 22, 2022
Accepted: May 15, 2022
Published: May 18, 2022

Abstract

Nile Delta which covers approximately 60,000 square kilometers represents the most important gas province in Egypt whereas its fields provide two-thirds of the gas production in Egypt. The Nile Delta province begins to display its hydrocarbon potentiality in the early 1960s. Nidoco field is located in the shallow water offshore Nile delta. Abu Madi formation (Messinian age) is the most important formation through all the section where it represents the main gas producing reservoirs in the Field. The production of the field is coming from two sand reservoir levels; Abu Madi level 2&3 which are characterized by fluvial-deltaic sandstones. The purpose of this paper is to perceive the Messinian gas bearing reservoirs and channelized sand distribution inside Abu Madi formation using seismic attributes and amplitude versus offset (AVO) technique. The results indicated that the seismic attributes and AVO aided to give a complete picture about the Messinian reservoirs distribution and characterization in the field. Also the results show that there are still promising locations of prospective Abu Madi Level 2&3 which are proposed to be drilled in the field.

Keywords

AVO, Nidoco Field, Abu Madi Formation, Seismic Attributes

1. Introduction

Nidoco field is located in the shallow water offshore Nile Delta, Egypt. The main producing reservoirs and target zones in the field belong to the Level 2&3 of the upper Messinian (Abu Madi formation). These Abu Madi Levels reservoirs consist mainly of continental deposits in a fluvial-deltaic environment (Figure 1).

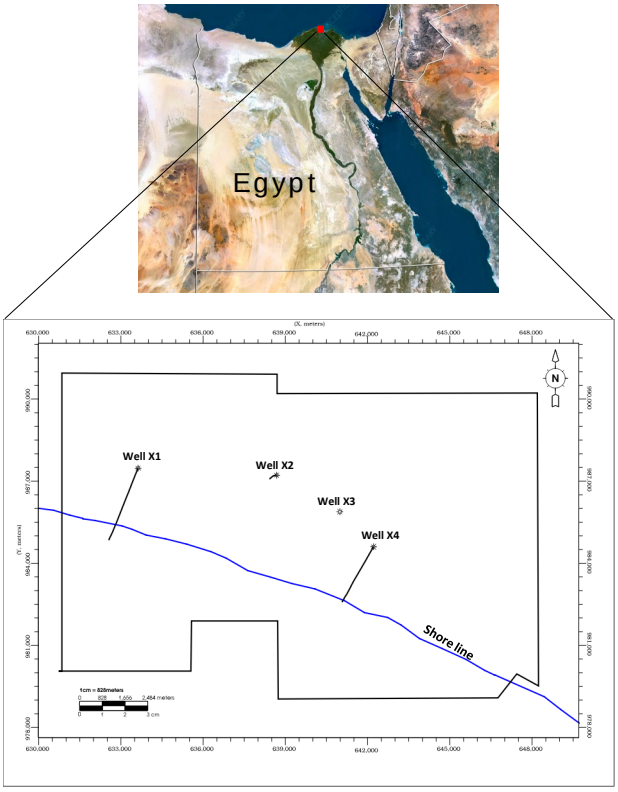

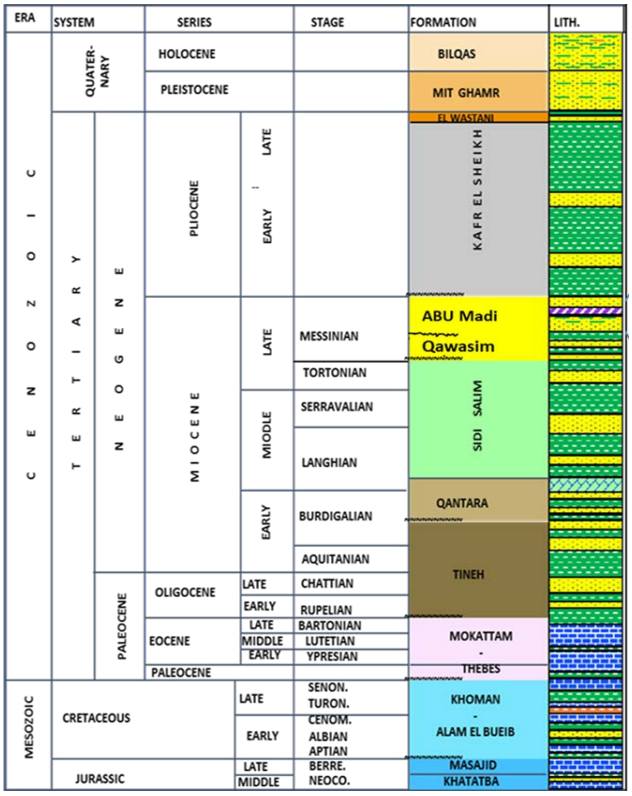

Figure 1. Location map of the study area (left), stratigraphic column for the Nile Delta (Matresu *et al.*, 2014) [1] (right).

The field was discovered in 1993 in the Level 3 of Abu Madi Formation as the main production reservoir. From 1994-1998 three exploratory and two development wells were drilled. In 2011 other well was drilled, with the aim to raise the decreasing production inside the development lease. In December 2012 its production from Level 3 was stopped due to presence of water. In May 2015 the onshore exploratory well drilled the first segment of the Nooros Prospect to reach the offshore target Abu Madi Level 2. The well encountered gas bearing sandstones of 60 meters in Upper Messinian reservoir level. In three months the well was completed, tested and put on production. It was followed by two appraisal wells located to drill two more segments of the Nooros prospect which proved to be gas discoveries. Then gas and condensate production from Nooros discovery has been further increased by additional development wells drilled in the field.

The main purposes of this paper are as follow:

- Interpreting the seismic data and extracting seismic attributes to have an idea about the structural and stratigraphic reservoir levels of Abu madi formation in the local study area.
- Investigating the AVO response of Messinian reservoirs in Nidoco field and generating scaled Poisson's ratio change attribute and crossplot for identifying the gas sand reservoirs (Messinian levels in Abu Madi formation).

2. Methodology

The first part of this research focuses on the interpretation of the available seis-

mic data to understand the different structures of Abu madi levels in the study area, and to identify the sand distribution by extracted seismic attributes. Well to seismic ties were also carried out to make a match between the gas zones in the well log data and the seismic data.

AVO gradient analysis is carried out to understand the AVO class of the gas proven anomalies and the prospective anomaly in the area. AVO attributes and crossplots also are created to comparing between the gas sands reservoirs and brine sands levels.

The methods can be summarized by a workflow chart (**Figure 2**).

2.1. Seismic Attributes

Vikesh (2013), defines an attribute as a quality, property, or characteristic of somebody or something. A seismic attribute is a measurement derived from seismic data, usually based on measurements of time, amplitude, frequency, and/or attenuation (Sheriff, 2002) [2]. They may be time-based (related to structure) or amplitude-based (related to stratigraphy and reservoir characterization). These attributes are used to visually enhance or isolate features of prediction.

To define the distribution of the channelized sand features in Abu Madi paleo-valley and to show the structure pattern in the study area, seismic attributes (structure maps and horizon amplitude) were extracted on the Abu Madi Level 2 and 3 picked horizons.

2.2. Amplitude Maps

Seismic amplitude is a post stack attribute which plays a major role in identifying lithology, geometry of sedimentary features and depositional setting. It is a measure of the contrast in properties between two layers. Maximum positive amplitude calculates the highest value of the amplitude.

2.3. Structure Maps

Structure map is a type of subsurface map whose contours represent the elevation of a particular formation, reservoir or geologic marker in space, such that folds, faults and other geologic structures. Time structure map is a plot of the two-way-time of seismic signal to the surface of the horizon. Time-structure map can be converted into depth-structure maps using velocity. According to Asquith and Gibson (1982) [3], a hydrocarbon reservoir is considered to be a potential prospect if they are trapped within structural traps.

2.4. AVO Application

The seismic response is affected by the physical properties of pore fluids in a porous rock containing those fluids (Hussein, M., *et al*., 2020) [4]. AVO analysis has become prominent in the DHI (Direct Hydrocarbons Indicator) aimed at characterizing the fluid content or the lithology of a possible reservoir and reducing the exploration drilling risk (Chenin, J., 2020) [5].

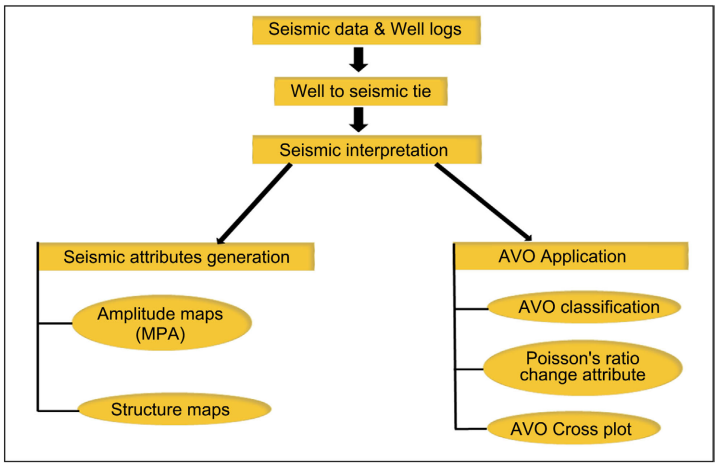

Figure 2. Simplified work flow chart.

The AVO technique has been developed by many researchers, such as Ostrander (1984) [6] and Rutherford and Williams (1989) [7] and all of them were started from the Aki-Richards equation (Stewart, R. R., 1990) [8], which is a practical approximation to the Zoeppritz equation (Zoeppritz, 1919) [9] for the reflection coefficient at the reflection interface.

The following formula is the two-term Shuey approximation to the Zoeppritz equations, which represents the angular dependence of P-wave reflection coefficients with two parameters: the AVO intercept (A) and the AVO gradient (B). In practice, the AVO intercept is a band-limited measure of the normal incidence amplitude, while the AVO gradient is a measure of amplitude variation with offset. Assuming appropriate amplitude calibration, A is the normal incidence reflection coefficient and B is a measure of offset-dependent reflectivity (Shuey, 1985) [10].

$$R(\theta) \approx A + B\sin^2\theta$$

where: θ is the incidence angle, $R(\theta)$ is the reflection coefficient at θ, A is the AVO intercept and B is the AVO gradient.

3. Results and Discussion

3.1. Amplitude and Structure Maps

Well to seismic tie was performed using the available logs of Well 3 and seismic data to study the phase and polarity of seismic data (**Figure 3**). The seismic data has a zero phase and European polarity. So the Abu Madi Level 2&3 were interpreted on the seismic sections in a right way. Since faults are very important in the petroleum exploration industry, they were picked on the full-angle stack seismic sections (**Figure 4**). These faults in this area are normal faults and have a generally N-S trend.

The Maximum positive amplitude is extracted from the full-angle stack seismic data in the time intervals from 10 ms above to 10 ms below each horizon of AML2 &3. The amplitude maps of AML 2&3 shows the sand distribution within the area which are characterized by fluvio-deltaic sandstones (**Figure 5**).

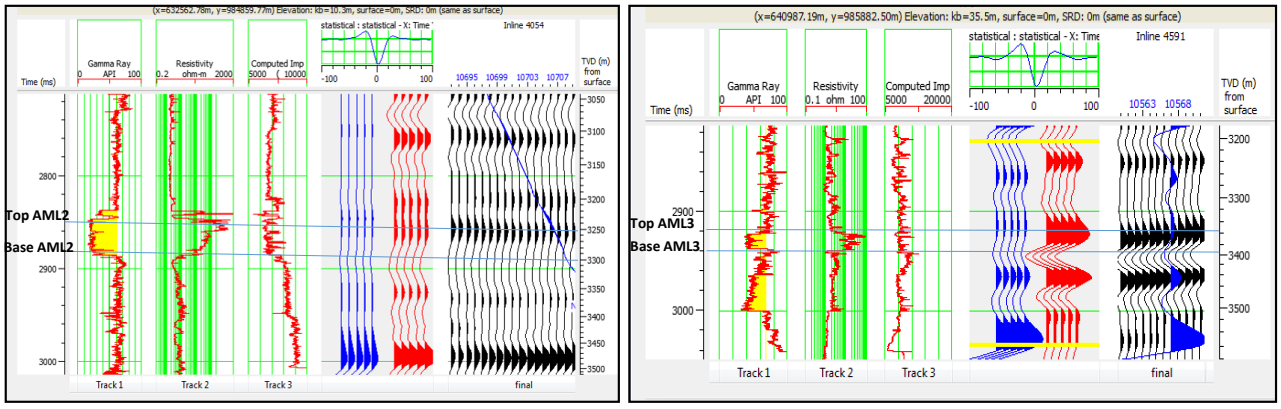

Figure 3. Well to seismic ties on well X3 (left) and well X1 (right).

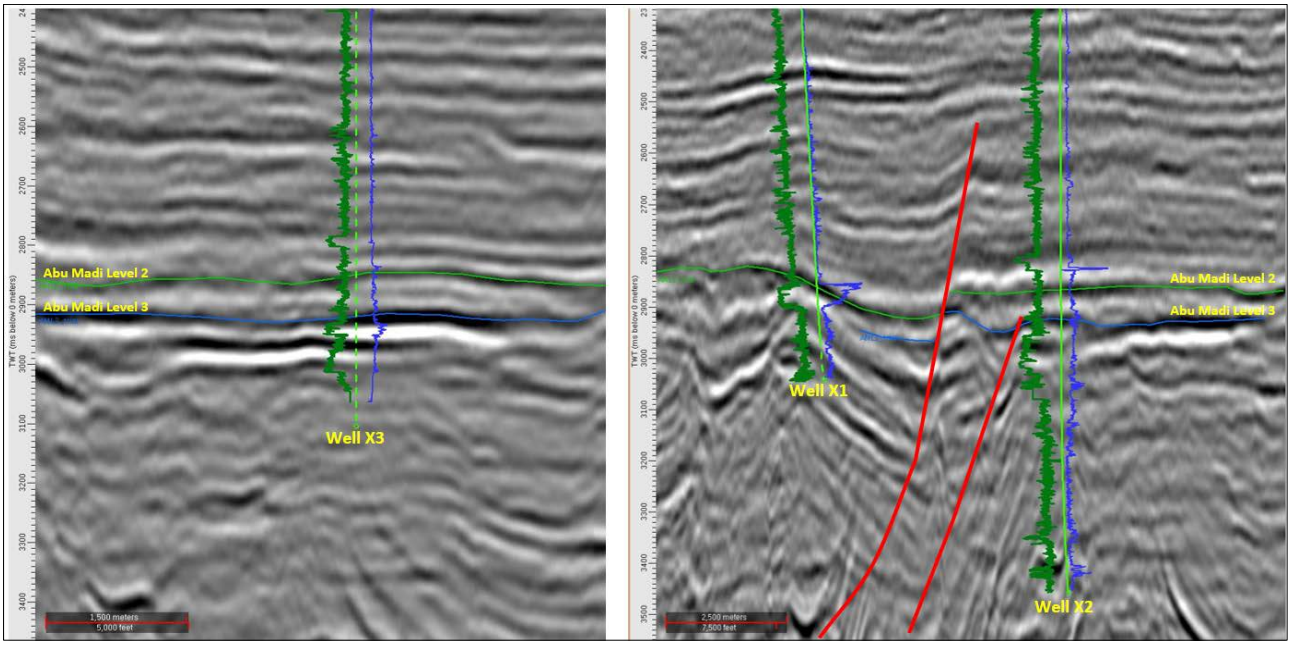

Figure 4. Interpreted horizon Abu Madi Level 2&3 across seismic sections from full angle stack volume.

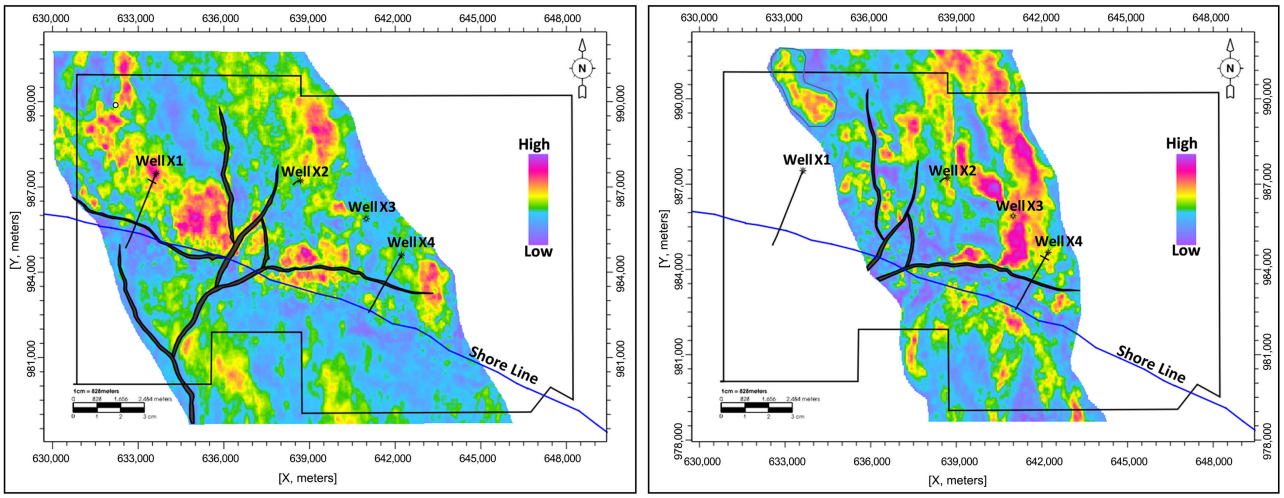

Figure 5. Maximum positive amplitude (MPA) maps on Abu Madi Level 2 and 3 with the fault polygons with proposal locations.

Figure 6 shows the depth maps of these Abu Madi levels after time to depth conversion. When amplitude maps are compared to structure, they may indicate a direct hydrocarbon indicator, or DHI. The figure shows that the AML 2&3 reservoirs are conformable with the high structure. Also there are suggested locations to be drilled as a new remaining potentiality.

3.2. AVO Classification

According to the AVO classification for gas sand reservoirs (Castagna and Swan 1998) [11], there are four classes for the classtic rocks. class I response is characterized by an increasing in impedance downward causing (decreasing in amplitude with increasing in incidence angle), class II has small normal incidence amplitude (+ or −), but the AVO leads to negative amplitudes at far offsets, class IIp where the zero incidence (or near offsets) is positive and therefore there is a polarity reversal at intermediate offsets, class III have large negative impedance contrast and negative gradient leads to increasing in amplitude with increasing in incidence angle, class IV has a large negative amplitude decreasing slightly with offset (Figure 7).

The reservoir sands of Abu Madi are characterized by acoustic impedance values that are lower than the encasing shale. Figure 8 highlights the AVO gradient analysis for the Abu Madi Level 2&3 gas anomalies. The prospective anomaly has the same AV response (AVO class III) as the gas bearing reservoirs anomalies in well X1 and X3.

3.3. Poisson's Ratio Change Attribute

Poisson's ratio is one of the best indicators for the presence of gas saturated sands. Scaled poisons ratio AVO attribute shows variation based on the fluid content of the reservoir. (Castagna, J. P., 2001 and Foster *et al.*, 2010) [12] [13] described that sands can have higher or lower acoustic impedance than surrounding shale, but gas sands have a lower poisons ratio than shale or brine sands. Ross (2002) [14] mentioned that this attribute works well for class II and III AVO responses. The derivative scaled Poisson's ratio attribute can use in identifying the gas bearing sands and the prospective anomaly in the study area (Figure 9).

3.4. AVO Crossplots

Castagna and Swan (1997) [15] show that the cross-plotting technique is the easiest method to derive the relationships between different variables. This technique is used in this paper to plot the AVO Intercept attribute on the X-axis and AVO gradient on the Y-axis.

The gas bearing anomalies and the prospective anomalies of Abu Madi Level 2&3 can be isolated from the background of the shale and brine sand and were plotted on the sections (Figure 10). The top of gas sand is in red color and the base of gas sand is in yellow color.

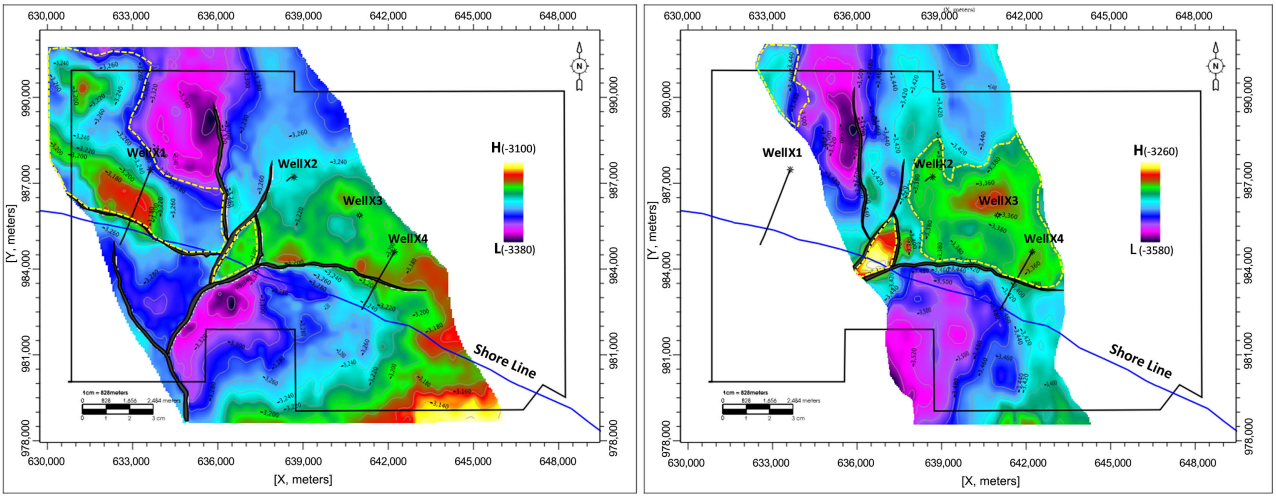

Figure 6. Depth structure maps on Abu Madi Level 2 and 3 with proposal locations, the reservoirs inside yellow polygon of high amplitude are conformable with high structure.

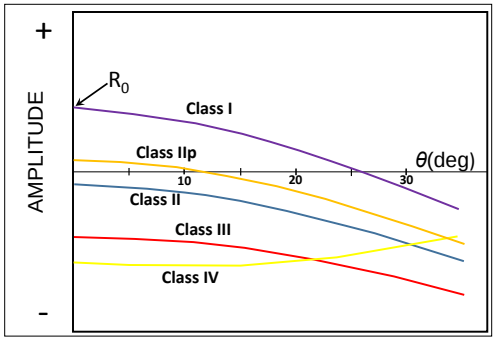

Figure 7. The classes of AVO response.

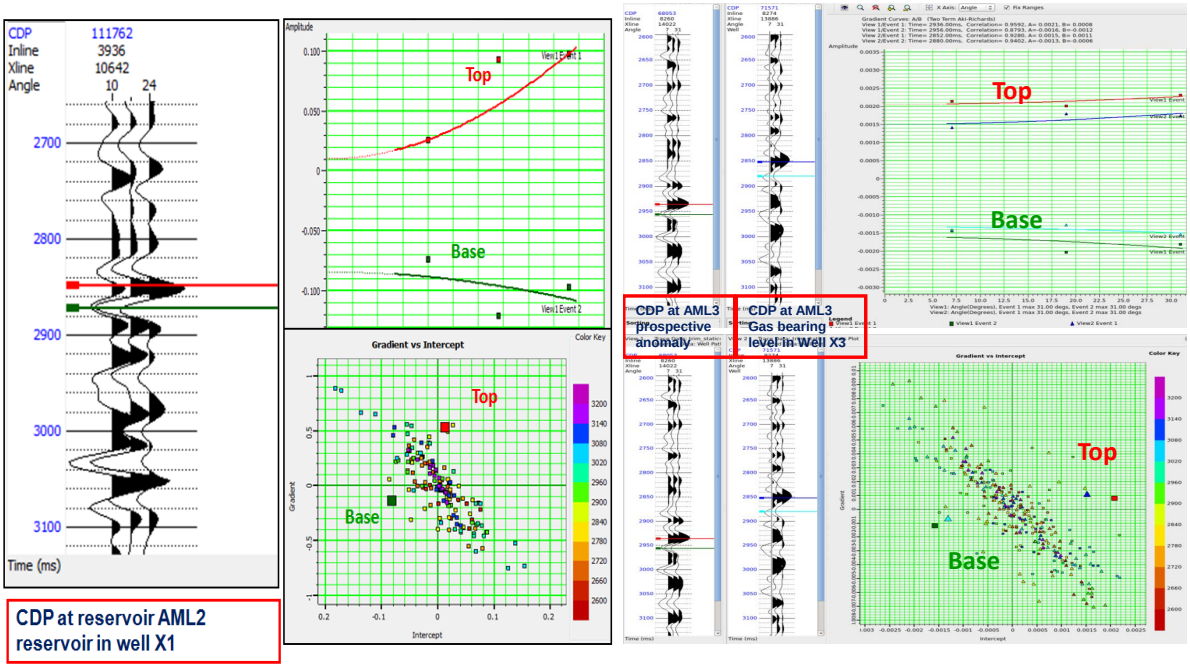

Figure 8. AVO gradient analyses highlight the comparison between the response of the gas bearing and the prospective anomalies.

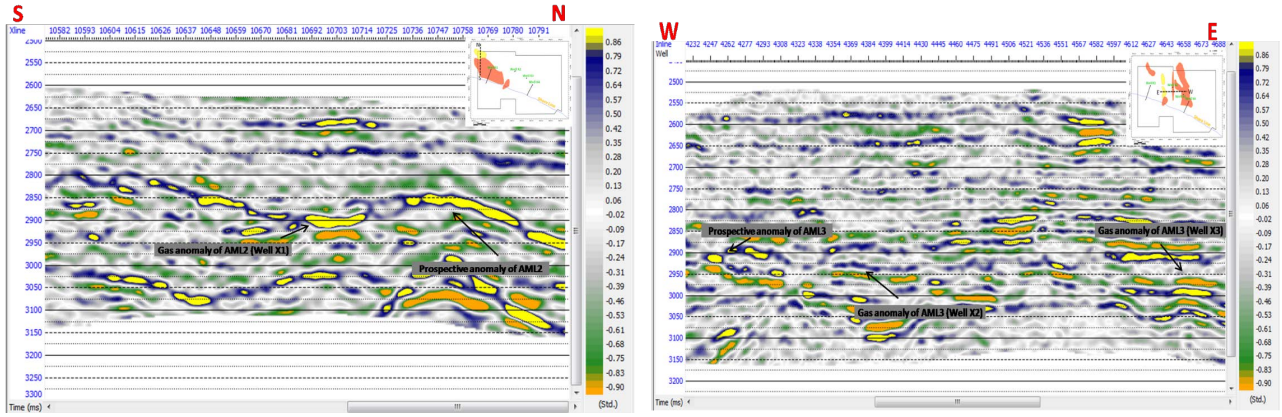

Figure 9. Scaled poison's ratio attributes for AML2&3 reservoirs and AML3 prospective anomaly.

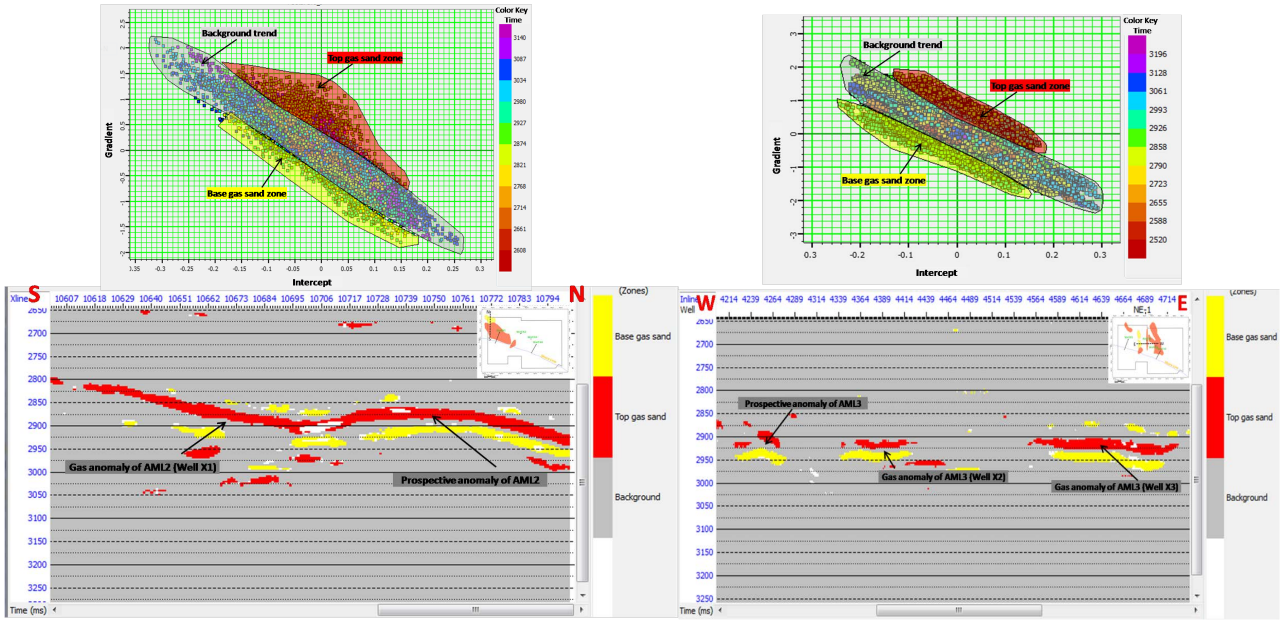

Figure 10. AVO crossplot with locating the results on the sections.

4. Conclusions

In conclusion, Seismic attributes are considered as a direct hydrocarbon indicator (DHI) whereas amplitude maps can aid to identify the sand deposits distribution which was characterized by the fluvial deposition environment of the Level 2 &3 in the Messenian section (Abu Madi formation) at Nidoco field. Also the integration of structure maps with the extracted amplitude maps may help to recognize the reservoirs in the study area. It can aid in locating a new proposal well in the field. The new prospective anomalies are related to Abu Madi Level 2&3.

The sand anomalies of Abu Madi Level 2&3 are classified as AVO class III. In addition AVO attributes and crossplotting of intercept and gradient can use to correlate the gas bearing sand anomalies with the prospective anomalies.

Seismic attributes (such as amplitude maps and structure maps) and the am-

plitude versus offset technique are considered as powerful techniques in validating the prospects before drilling. So it is recommended to use these techniques in the study area.

Acknowledgements

The authors wish to thank Egyptian General Petroleum Corporation (EGPC) and Belayim Petroleum Company (PETROBEL) for providing the seismic data, well logs, and other relevant data. This work is original. No conflict of interest, No fund for my work

Conflicts of Interest

The authors declare no conflicts of interest regarding the publication of this paper.

References

[1] Matresu, J., Bettazzoli, P., Bertello, F., Nassar, M., Bricchi, G., Talaat, A. and Elsayed, A.Z.S. (2014) The Nooros Discovery. Offshore Central.

[2] Sheriff, R.E. (2002) Encyclopedic Dictionary of Applied Geophysics. Society of Exploration Geophysicists. https://doi.org/10.1190/1.9781560802969

[3] Asquith, G.B. and Gibson, C.R. (1982) Basic Well Log Analysis for Geologists (Vol. 3). American Association of Petroleum Geologists, Tulsa. https://doi.org/10.1306/Mth3425

[4] Hussein, M., El-Ata, A.A. and El-Behiry, M. (2020) AVO Analysis Aids in Differentiation between False and True Amplitude Responses: A Case Study of El Mansoura Field, Onshore Nile Delta, Egypt. *Journal of Petroleum Exploration and Production Technology*, **10**, 969-989. https://doi.org/10.1007/s13202-019-00806-2

[5] Chenin, J. (2020) Examining Seismic Amplitude Responses of Gaseous Media Using Unsupervised Machine Learning. Doctoral Dissertation, University of Oklahoma, Norman.

[6] Ostrander, W.J. (1984) Plane-Wave Reflection Coefficient for Gas Sand at Non-Normal Angles of Incidence. *Geophysics*, **49**, 1637-1648. https://doi.org/10.1190/1.1441571

[7] Rutherford, S.R. and Williams, R.H. (1989). Amplitude-versus-Offset Variations in Gas Sands. *Geophysics*, **54**, 680-688. https://doi.org/10.1190/1.1442696

[8] Stewart, R.R. (1990) Joint P and P-SV Inversion. *The CREWES Project Research Report*, **2**, 112-115.

[9] Zoeppritz, K. (1919) Joachim Ritter & Johannes Schweitzer. Part C. Biography of Angenheister and of Geiger, Wiechert's Bibliography, and Biographical Notes, 34.

[10] Shuey, R.T. (1985) A Simplification of the Zoeppritz Equations. *Geophysics*, **50**, 609-614. https://doi.org/10.1190/1.1441936

[11] Castagna, J.P., Swan, H.W. and Foster, D.J. (1998) Framework for AVO Gradient and Intercept Interpretation. *Geophysics*, **63**, 948-956. https://doi.org/10.1190/1.1444406

[12] Castagna, J.P. (2001) Recent Advances in Seismic Lithologic Analysis. *Geophysics*, **66**, 42-46. https://doi.org/10.1190/1.1444918

[13] Foster, N.E.V. and Zatorre, R.J. (2010) Cortical Structure Predicts Success in Performing Musical Transformation Judgments. *NeuroImage*, **53**, 26-36. https://doi.org/10.1016/j.neuroimage.2010.06.042

[14] Ross, C.P. (2002) Comparison of Popular AVO Attributes, AVO Inversion, and Calibrated AVO Predictions. *The Leading Edge*, **21**, 244-252. https://doi.org/10.1190/1.1463776

[15] Castagna, J.P. and Swan, H.W. (1997) Principles of AVO Crossplotting. *The Leading Edge*, **16**, 337-344. https://doi.org/10.1190/1.1437626